FUZZY LOGIC BASED QUADROTOR FLIGHT CONTROLLER

Syed Ali Raza and Wail Gueaieb

School of Information Technology and Engineering, University of Ottawa
800 King Edward Avenue, Ottawa, ON, Canada

Abstract: Quadrotor unmanned aerial vehicles (UAVs) have gained a lot of research interest in the past few years, due to the clear advantages posed by their vertical take-off and landing (VTOL), hovering capability, and slow precise movements. These characteristics make quadrotors an ideal candidate for applications that require traversing through difficult environments with many obstacles. Belonging to the helicopter rotorcraft class, quadrotors are highly nonlinear systems that are difficult to stabilize. This paper proposes a fuzzy logic based flight controller for an autonomous quadrotor. Two types of fuzzy logic controllers are implemented. The developed flight controllers are tested in a quadrotor simulator and simulation results are presented to demonstrate the performance of each controller. The controllers performances are also benchmarked against conventional control based techniques such as input-output linearization, backstepping and sliding mode control. In comparison with other conventional control techniques mostly designed for indoor applications, the proposed fuzzy logic based controllers showed satisfactory control of the quadrotor in the presence of various disturbances such as sensor noise and high wind conditions.

NOMENCLATURE

The following notations are used in the paper:
$\mathcal{F}_n$ represents the reference frame where the subscript $n \in \{i, b, v, \phi, \theta\}$.
$()_{\mathcal{F}_n}$ represents a point or a vector in reference frame $\mathcal{F}_n$.
$\dot{(\,)}, \ddot{(\,)}$ represent first and second time derivatives, respectively.
$R_{\mathcal{F}_1}^{\mathcal{F}_2} \in \mathbb{R}^{n \times n}$ is the rotation matrix that maps frame $\mathcal{F}_1$ to frame $\mathcal{F}_2$.
$s\theta = \sin\theta$, $c\theta = \cos\theta$.
I is the identity matrix.
COG is the quadrotor's center of gravity.
$P^T = [p_x \ p_y \ p_z]$ is the position of the quadrotor's COG.
M is the mass of quadrotor (including the motors).
m is the mass of one motor.
l is the length of the arms of quadrotor.
$J^T = [j_x \ j_y \ j_z]$ is the moment of inertia vector of the quadrotor.
ϕ, θ, ψ are the quadrotor's roll, pitch, and yaw angles, respectively.
$\Omega^T = [\phi \ \theta \ \psi]$ is the quadrotor's orientation vector.
K_T and K_τ are motor constants.
$T_{motor}, \tau_{motor}, \text{PWM}_{motor}$ are thrust, drag and PWM value for $motor \in \{f, r, b, l\}$, the subscripts f, r, b,

and l, denote front, right, back, and left, motors respectively.

1 INTRODUCTION

The motivation for employing robots in search and rescue operations is multifaceted. However, the technology is still in its infancy and there are many issues which need to be addressed. Search and rescue missions, as well as simulations, have demonstrated several areas in which robot contributions need to be improved (Fincannon et al., 2004). Advances in computing, MEMS inertial measurement sensors, and communications technology make it possible to achieve autonomous performance and coordination of these vehicles in test environments (Waslander et al., 2005). But, achieving complete autonomous performance in real environments is a milestone yet to be reached.

A quadrotor, as depicted in Figure 1, is a rotary wing UAV, consisting of four rotors located at the ends of a cross structure. By varying the speeds of each rotor, the flight of the quadrotor is controlled. Quadrotor vehicles possess certain essential characteristics, which highlight their potential for use in search and rescue applications. Characteristics that
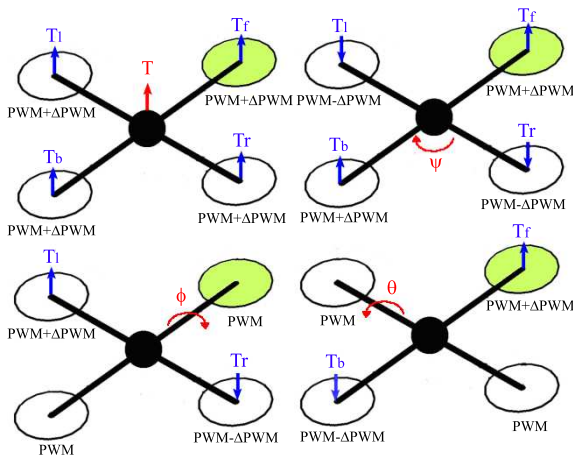
Figure 1: Conceptual diagram of the quadrotor.

provide a clear advantage over other flying UAVs include their Vertical Take Off and Landing (VTOL) and hovering capability, as well as their ability to make slow precise movements. There are also definite advantages to having a four rotor based propulsion system, such as a higher payload capacity, and impressive maneuverability, particularly in traversing through an environment with many obstacles, or landing in small areas.

The quadrotor is an under-actuated system, in that the four forces applied on the body result in movements achieved in six degrees. Being a non-linear system it offers an interesting and challenging control problem. The flight controller is responsible for achieving the desired attitude, i.e. the orientation (roll, pitch and yaw angles) of the quadrotor and also the desired position of quadrotor in the space.

In past few years, a lot of research has already been conducted on the modeling and control of a quadrotor. Many control techniques are proposed in the literature, however, their primary focus is mostly for indoor flight control and therefore does not account for uncertainties. Lyapunov stability theory is used for stabilization and control of the quadrotor in (Bouabdallah et al., 2004a) (Dzul et al., 2004). Conventional PD^2 feedback, and PID structures are used for simpler implementation of control laws and comparison with LQR based optimal control theory is presented in (Tayebi and McGilvray, 2006) (Bouabdallah et al., 2004b). Backstepping control is also proposed with the drawback of higher computational loads in (Guenard et al., 2005). Visual feedback is used in many cases using onboard or offboard cameras for pose estimation by (Altug et al., 2002) (Guenard et al., 2008). And finally some fuzzy logic based control techniques (Coza and Macnab, 2006), neural networks (Tarbouchi et al., 2004) and reinforcement learning (Waslander et al., 2005).

Fuzzy logic based control offers a great advantage over conventional control, specifically in dealing with nonlinear systems with uncertainties. In this paper two fuzzy logic based flight controllers for an autonomous quadrotor are proposed. Implementation of the proposed control is carried out using Mamdani and Sugeno fuzzy inferencing methodologies. The advantage of the proposed methodology over other conventional methods is the ability to achieve stable flight control under disturbances that are common in outdoor environments. Also the implementation is lighter in terms of computational loads as compared to techniques such as backstepping control. Both controllers are simulated and their performances are benchmarked against various conventional control techniques. The results are presented to show the satisfactory performance of the proposed fuzzy logic based controllers despite the presence of various disturbances, such as sensor noise and high wind conditions.

2 QUADROTOR'S KINEMATICS AND DYNAMICS

The flight behavior of a quadrotor is determined by the speeds of each of the four motors, as they vary in concert, or in opposition with each other. Hence, a mathematical representation of the system can be used to predict the position and orientation of the quadrotor, based on its inputs. The same can further be used to develop a control strategy, whereby manipulating the speeds of individual motors results in the achievement of the desired motion. To derive a mathematical model of the quadrotor, we need to define its kinematics and dynamics. The kinematics of the quadrotor gives a relation between the position of the vehicle in the inertial frame, and its velocity in the body frame. The dynamics of the quadrotor provides the relation between the applied body forces and the resulting accelerations.

Three frames of reference are adopted;

1. The inertial frame, $\mathcal{F}_i = (\overrightarrow{x_i}, \overrightarrow{y_i}, \overrightarrow{z_i})$, is an earth-fixed coordinate system with the origin located on the ground, for example, at the base station. By convention, the x-axis points towards the north, the y-axis points towards the east, and the z-axis points towards the center of the earth.

2. The body frame, $\mathcal{F}_b = (\overrightarrow{x_b}, \overrightarrow{y_b}, \overrightarrow{z_b})$, with its origin located at the center of gravity (COG) of the quadrotor, and its axes aligned with the quadrotor structure such that the x-axis $\overrightarrow{x_b}$ is along the arm

with front motor, the y-axis $\overrightarrow{y_b}$ is along the arm with right motor, and the z-axis $\overrightarrow{z_b} = \overrightarrow{x_b} \times \overrightarrow{y_b}$.

3. The vehicle frame, $\mathcal{F}_v = (\overrightarrow{x_v}, \overrightarrow{y_v}, \overrightarrow{z_v})$, is the inertial frame with the origin located at the COG of the quadrotor. The vehicle frame has two variations, $\mathcal{F}_\phi$ and $\mathcal{F}_\theta$. $\mathcal{F}_\phi$, is the vehicle frame, $\mathcal{F}_v$, rotated about its z-axis $\overrightarrow{z_v}$ by an angle ψ so that $\overrightarrow{x_v}$ and $\overrightarrow{y_v}$ are aligned with $\overrightarrow{x_b}$ and $\overrightarrow{y_b}$, respectively. $\mathcal{F}_\theta$ is the $\mathcal{F}_\phi$ frame rotated about its y-axis, $\overrightarrow{y_\phi}$, by a pitching angle, θ, such that $\overrightarrow{x_\phi}$ and $\overrightarrow{z_\phi}$ are aligned with $\overrightarrow{x_b}$ and $\overrightarrow{z_b}$, respectively.

With the knowledge of the inertial frame position state variables P_i and the body frame speed state variables $\dot{P}_{\mathcal{F}_b}$, the translational motion relationship is derived as

$$\begin{bmatrix} \dot{p}_x \\ \dot{p}_y \\ -\dot{p}_z \end{bmatrix}_{\mathcal{F}_i} = \left[R^{\mathcal{F}_b}_{\mathcal{F}_v} \right]^T \begin{bmatrix} \dot{p}_x \\ \dot{p}_y \\ \dot{p}_z \end{bmatrix}_{\mathcal{F}_b}$$

where $\left[R^{\mathcal{F}_b}_{\mathcal{F}_v} \right]^T \in \mathbb{R}^{3 \times 3}$ is the rotation that maps frame $\mathcal{F}_b$ to frame $\mathcal{F}_v$ and is defines by

$$\left[R^{\mathcal{F}_b}_{\mathcal{F}_v} \right]^T = \begin{bmatrix} c\theta c\psi & s\phi s\theta c\psi - c\phi s\psi & c\phi s\theta c\psi + s\phi s\psi \\ c\theta s\psi & s\phi s\theta s\psi + c\phi c\psi & c\phi s\theta s\psi - s\phi c\psi \\ -s\theta & s\phi c\theta & c\phi c\theta \end{bmatrix}$$

The rotational motion relationship is also derived using the state variables involved:

$$\begin{bmatrix} \dot{\phi} \\ \dot{\theta} \\ \dot{\psi} \end{bmatrix}_{\mathcal{F}_v} = \begin{bmatrix} 1 & s\phi \tan\theta & c\phi \tan\theta \\ 0 & c\phi & -s\phi \\ 0 & s\phi/c\theta & c\phi/c\theta \end{bmatrix} \begin{bmatrix} \dot{\phi} \\ \dot{\theta} \\ \dot{\psi} \end{bmatrix}_{\mathcal{F}_b}.$$

The quadrotor's dynamics is obtained by applying Newton-Euler formulation.

$$\begin{bmatrix} MI_{3\times3} & 0 \\ 0 & I_{3\times3} \end{bmatrix} \begin{bmatrix} \ddot{P}_{\mathcal{F}_b} \\ \dot{\Omega}_{\mathcal{F}_b} \end{bmatrix} + \begin{bmatrix} \dot{\Omega}_{\mathcal{F}_b} M \dot{P}_{\mathcal{F}_b} \\ \dot{\Omega}_{\mathcal{F}_b} I \Omega_{\mathcal{F}_b} \end{bmatrix} = \begin{bmatrix} F_{\mathcal{F}_b} \\ \tau_{\mathcal{F}_b} \end{bmatrix}$$

where $F^T = [f_x \ f_y \ f_z]$ and $\tau^T = [\tau_\phi \ \tau_\theta \ \tau_\psi]$ are external force and torque vectors applied on the quadrotor's COG. τ_ϕ, τ_θ, and τ_ψ are the roll, pitch and yaw torques respectively. Hence, the models for the translational and rotational motion are

$$\begin{bmatrix} \ddot{p}_x \\ \ddot{p}_y \\ \ddot{p}_z \end{bmatrix}_{\mathcal{F}_b} = \begin{bmatrix} \dot{\psi}\dot{p}_y - \dot{\theta}\dot{p}_z \\ \dot{\phi}\dot{p}_z - \dot{\psi}\dot{p}_x \\ \dot{\theta}\dot{p}_x - \dot{\phi}\dot{p}_y \end{bmatrix}_{\mathcal{F}_b} + \frac{1}{M} \begin{bmatrix} f_x \\ f_y \\ f_z \end{bmatrix}_{\mathcal{F}_b}$$

$$\begin{bmatrix} \ddot{\phi} \\ \ddot{\theta} \\ \ddot{\psi} \end{bmatrix}_{\mathcal{F}_b} = \begin{bmatrix} \frac{j_y - j_z}{j_x}\dot{\theta}\dot{\psi} \\ \frac{j_z - j_x}{j_y}\dot{\phi}\dot{\psi} \\ \frac{j_x - j_y}{j_z}\dot{\phi}\dot{\theta} \end{bmatrix}_{\mathcal{F}_b} + \begin{bmatrix} \frac{1}{j_x}\tau_\phi \\ \frac{1}{j_y}\tau_\theta \\ \frac{1}{j_z}\tau_\psi \end{bmatrix}_{\mathcal{F}_b}$$

where $j_x = j_y = j_z = \frac{2Mr^2}{5} + 2l^2m$. The moment of inertia is calculated by assuming the COG of the quadrotor as a sphere of radius r and mass M. Also,

each motor is represented by a point mass m with arms length l. The relationship between the quadrotor's overall thrust and drag produced by individual thrust of the motors is defined by

$$T = T_f + T_r + T_b + T_l \ , \ \tau_\psi = (\tau_f + \tau_b) - (\tau_r + \tau_l)$$
$$\tau_\phi = l(T_l - T_r) \ , \ \tau_\theta = l(T_f - T_b)$$

with

$$T_{motor} = K_T \times \text{PWM}_{motor} \text{ and } \tau_{motor} = K_\tau \times \text{PWM}_{motor}$$

for $motor \in \{f, r, b, l\}$. In matrix form, we get

$$\begin{bmatrix} \text{PWM}_f \\ \text{PWM}_r \\ \text{PWM}_b \\ \text{PWM}_l \end{bmatrix} = G \times \begin{bmatrix} T \\ \tau_\phi \\ \tau_\theta \\ \tau_\psi \end{bmatrix}$$

where

$$G = \begin{bmatrix} K_T & K_T & K_T & K_T \\ 0 & -l \times K_T & 0 & l \times K_T \\ l \times K_T & 0 & -l \times K_T & 0 \\ -K\tau & K\tau & -K\tau & K\tau \end{bmatrix}^{-1}.$$

Including the forces and torques acting on the system, the equations of motion become as defined in (1), with g being the gravitational force.

3 FLIGHT CONTROLLER DESIGN

Using the knowledge of the quadrotor's behavior from its equations of motion, a rule base is developed, which serves as a starting point for developing the fuzzy logic control strategy. These IF-THEN rules will later be combined to form a fuzzy controller, where fuzzy logic is used in a direct control scheme applied for the flight control of the quadrotor.
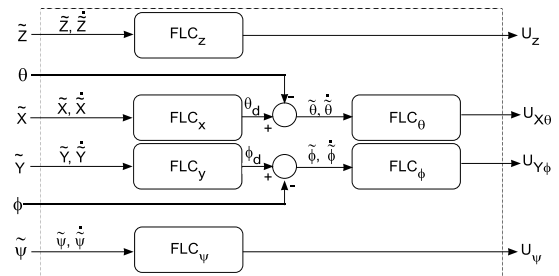

Figure 2: Block diagram of fuzzy logic based flight controller.

For attitude control, three fuzzy controllers are designed to control the quadrotor's roll (ϕ), pitch (θ)

$$\begin{bmatrix} \ddot{p}_x \\ \ddot{p}_y \\ \ddot{p}_z \end{bmatrix}_{\mathcal{F}_b} = \begin{bmatrix} \dot{\psi}\dot{p}_y - \dot{\theta}\dot{p}_z \\ \dot{\phi}\dot{p}_z - \dot{\psi}\dot{p}_x \\ \dot{\theta}\dot{p}_x - \dot{\phi}\dot{p}_y \end{bmatrix}_{\mathcal{F}_b} + \begin{bmatrix} -gs\theta \\ gc\theta s\phi \\ gc\theta c\phi \end{bmatrix} + \begin{bmatrix} 0 \\ 0 \\ \frac{-f_z}{M} \end{bmatrix} \quad , \quad \begin{bmatrix} \ddot{\phi} \\ \ddot{\theta} \\ \ddot{\psi} \end{bmatrix}_{\mathcal{F}_b} = \begin{bmatrix} \frac{j_y - j_z}{j_x}\dot{\theta}\dot{\psi} \\ \frac{j_z - j_x}{j_y}\dot{\phi}\dot{\psi} \\ \frac{j_x - j_y}{j_z}\dot{\phi}\dot{\theta} \end{bmatrix}_{\mathcal{F}_b} + \begin{bmatrix} \frac{1}{j_x}\tau_\phi \\ \frac{1}{j_y}\tau_\theta \\ \frac{1}{j_z}\tau_\psi \end{bmatrix}_{\mathcal{F}_b} \quad (1)$$

and yaw (ψ) angles. Here FLC_ϕ and FLC_θ fuzzy controllers are implemented in order to achieve attitude stabilization. Three fuzzy controllers are further designed for controlling the quadrotor's position. All the six fuzzy controllers, as depicted in Figure 2, have the same structure with two inputs and one output. The inputs are the error e, which is the difference between the desired and the actual state normalized to the interval $[-1, +1]$, and the error rate $\dot{e}$ normalized to the interval $[-3, +3]$. Three membership functions are used to fuzzify e, $\dot{e}$, and the output U: $\mu_N(e) = \text{trapezoid}(-1, -0.15, 0)$, $\mu_Z(e) = \text{triangle}(-0.15, 0, 0.15)$, $\mu_P(e) = \text{trapezoid}(0, 0.15, 1)$, $\mu_N(\dot{e}) = \text{trapezoid}(-3, -1.5, 0)$, $\mu_Z(\dot{e}) = \text{triangle}(-1.5, 0, 1.5)$, $\mu_P(\dot{e}) = \text{trapezoid}(0, 1.5, 3)$, $\mu_N(U) = \text{trapezoid}(-1, -0.85, 0)$, $\mu_Z(U) = \text{triangle}(-0.1, 0, 0.1)$, $\mu_P(U) = \text{trapezoid}(0, 0.85, 1)$.

A unified rule base comprising nine IF-THEN rules is developed for all the controllers. The developed rules are presented in Table 1.

Table 1: The rule base of the fuzzy controller.

		e		
		N	Z	P
	N	N	N	Z
$\dot{e}$	Z	N	Z	P
	P	Z	P	P

For the fuzzy controller to be independent of the quadrotor's parameters, the input and output signals of the designed fuzzy logic controllers are pre-processed and post-processed, respectively. The pre-processing process calculates the error e and error rate $\dot{e}$ and normalize them accordingly. The post-processing process calculates the individual motor PWM values by combining the outputs from the fuzzy logic controllers and adding a priori-defined offset to counter balance the weight of the quadrotor. The PWM value of each motor is then computed as follows:

$$PWM_f = Sat(U_Z + U_{X\theta} - U_\psi + \text{Offset})$$
$$PWM_r = Sat(U_Z + U_{Y\phi} + U_\psi + \text{Offset})$$
$$PWM_b = Sat(U_Z - U_{X\theta} - U_\psi + \text{Offset})$$
$$PWM_l = Sat(U_Z - U_{Y\phi} + U_\psi + \text{Offset})$$

Being independent of the plant's parameters sets the pure fuzzy controllers apart from the conventional control systems, which depends on the plant's parameters. The fuzzy controllers are designed in light of the behaviors extracted from the mathematical model of the quadrotor, whereas conventional control techniques are designed using the mathematical model of the plant. Any change in the plant dynamics or parameters results in the failure of such conventional control systems. In such situations, fuzzy systems are advantageous over conventional control techniques.

Two different fuzzy inference procedures are implemented: (i) a Mamdani fuzzy model, and (ii) a Takagi-Sugeno-Kang (TSK) fuzzy model. The Mamdani fuzzy inference method uses a min-max operator for the aggregation and centroid of area method for defuzzification. One problem with the designed Mamdani fuzzy control is the high computational burden associated to it when implemented on an embedded system. To alleviate this problem, a zero order Sugeno fuzzy model is implemented. In this model, the output membership functions of the Mamdani type FLC are replaced with fuzzy singletons $N = -1$, $Z = 0$ and $P = +1$.

4 NUMERICAL RESULTS

To test the proposed fuzzy flight controllers, and study their performances, a simulation environment is developed. The desired inputs from the user are the translatory coordinates $P_{\mathcal{F}_i}$ with respect to the inertial frame, and the yaw angle ψ. The pitch and roll angles are set to zero for achieving the desired attitude stabilization, as shall be shown later.

To make the simulations more realistic, sensory noise and environmental disturbances such as winds are also taken into account. Different wind conditions are generated based on the actual data from Canada Weather Statistics, representing high, medium and low wind conditions (Statistics, 2009). The angular accelerations $\ddot{\phi}$, $\ddot{\theta}$, and $\ddot{\psi}$ are degraded with a white noise and then used as a feedback to the fuzzy controller.

Several experiments are conducted on the two designed fuzzy controllers. Due to the space limitation, only three experiments are presented here. The controllers performances are benchmarked against those of similar control schemes found in the literature. The values used as the quadrotor's dynamic
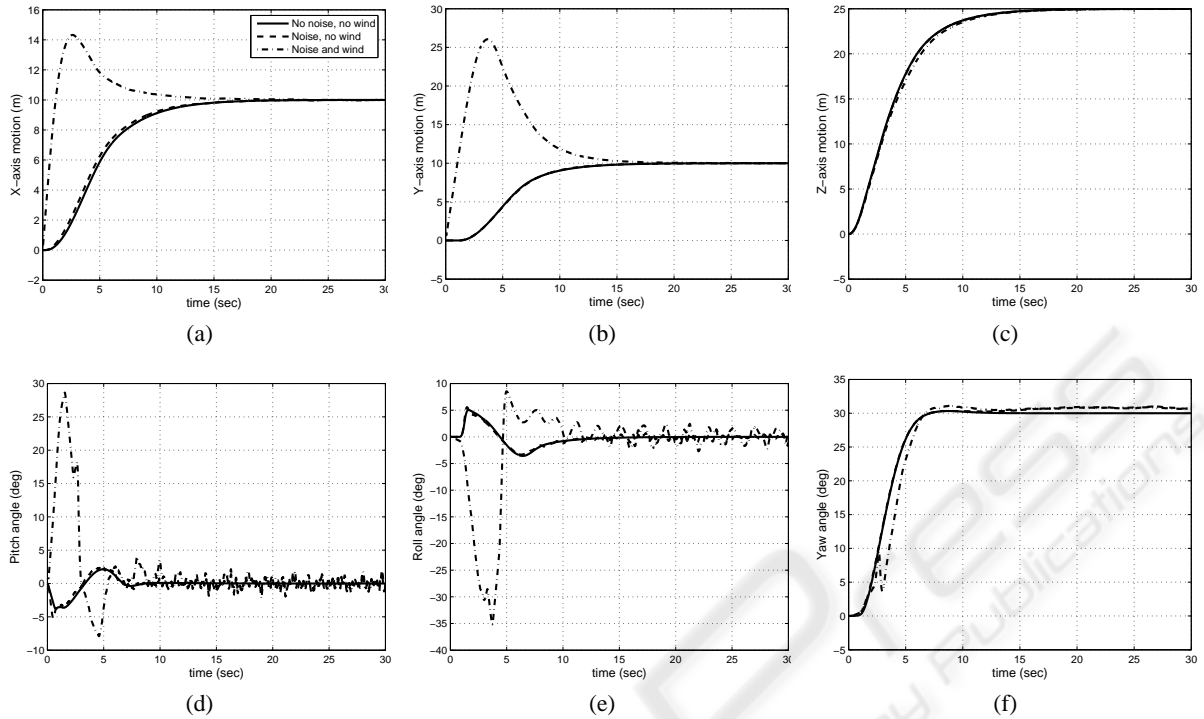
Figure 3: Experiment 1, Mamdani FLC's performance with and without disturbances. Quadrotor states: (a) x-axis; (b) y-axis; (c) z-axis (altitude); (d) pitch (θ); (e) roll (ϕ); and (f) yaw (ψ).

parameters are: $M = 1.56$ Kg, $l = 0.3$ m, $J_x = J_y = 0.08615$ Kg·m^2, $J_z = 0.1712$ Kg·m^2, $K_T = 5.45$, $K_{tau} = 0.0549$, Offset $= Mg/(4K_T) = 0.7018$.

In our first experiment the system's initial states are set to zero and the desired quadrotor's position and orientation are $P_{\mathcal{F}_i}^T = [10, 10, 25]$ m and $\Omega_{\mathcal{F}_i}^T = [0, 0, 30]$ degrees. The purpose of the experiment is to show the performance of both controllers under different disturbance conditions. The experiment is repeated three times for each controller, first time without any disturbances, second time with sensor noise only, and third time with sensor noise and medium north and east wind of $10m/s$. The experimental results presented in Figures 3 and 4, demonstrate the ability of both controllers to perform satisfactorily despite the presence of sensor noise and wind disturbances. The Mamdani fuzzy controller converges to the desired states relatively faster than the Sugeno fuzzy controller, however Sugeno shows better attitude stabilization, specially in the presence of the sensory noise and wind disturbances. The yaw angle drift under wind disturbance is clearly visible in the Sugeno results.

In second experiment, the position and attitude stabilization of the proposed controllers are benchmarked against feedback linearization based conventional control technique, where a series of mode-based, feedback linearizing controllers are implemented for the stabilization and control of a quadrotor (Altug et al., 2002). The system's initial states are considered to be $P_{\mathcal{F}_i}^T = [40, 20, 60]$ m and $\Omega_{\mathcal{F}_i}^T = [45, -45, 0]$ degrees. In the presence of sensor noise and winds, the system is supposed to stabilize all the states back to zero. The experimental results are depicted in Figures 5 and 6. The stabilization achieved by both proposed fuzzy controllers converge to the desired state faster than the feedback linearization technique. It is worth pointing out that the controller proposed in (Altug et al., 2002) did not consider any type of noise or external disturbances.

The third experiment benchmarks the proposed fuzzy controllers with simulation results of a backstepping controller tuned for optimized nonlinear control of a tethered quadrotor (Bouabdallah et al., 2004b). The backstepping control offers high robustness against large disturbances as compared to the feedback linearization technique which is clear from the results. To test the attitude stabilization of the proposed fuzzy controllers, the system is initialized with severe rotational angles $\Omega_{\mathcal{F}_i}^T = [45, 45, 45]$ degrees. Again, the sensory noise and winds are introduced as disturbances. The experimental results show
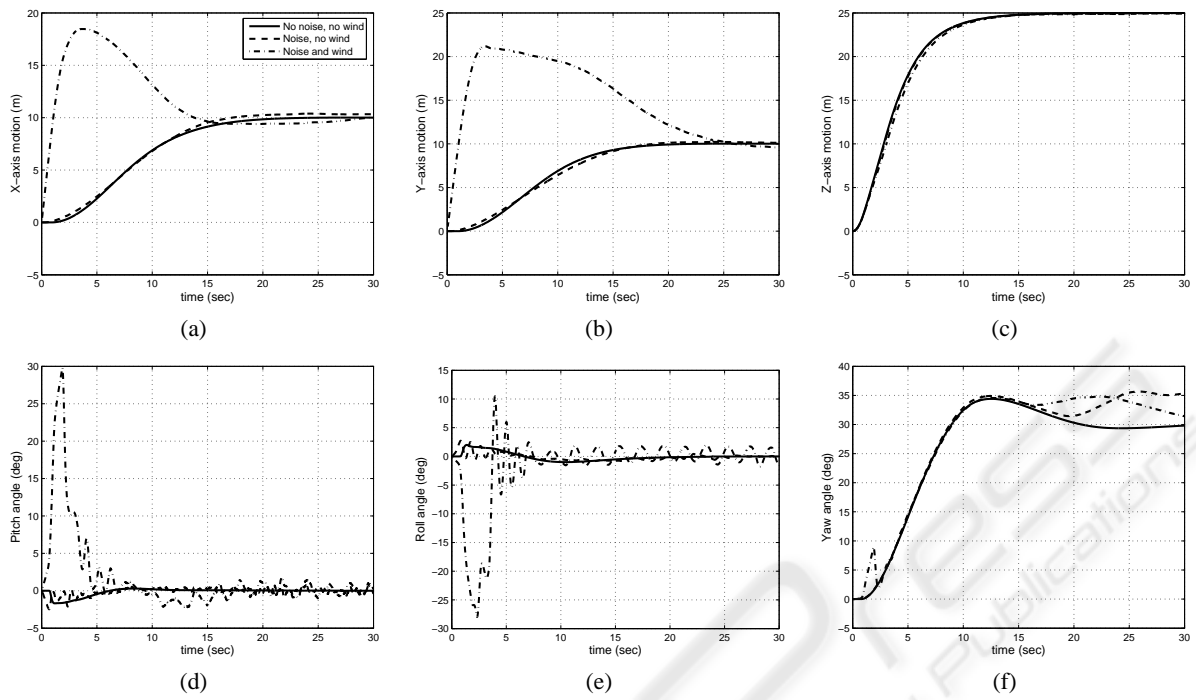
Figure 4: Experiment 1, Sugeno FLC's performance with and without disturbances. Quadrotor states: (a) x-axis; (b) y-axis;; (c) z-axis (altitude); (d) pitch (θ); (e) roll (ϕ); and (f) yaw (ψ).
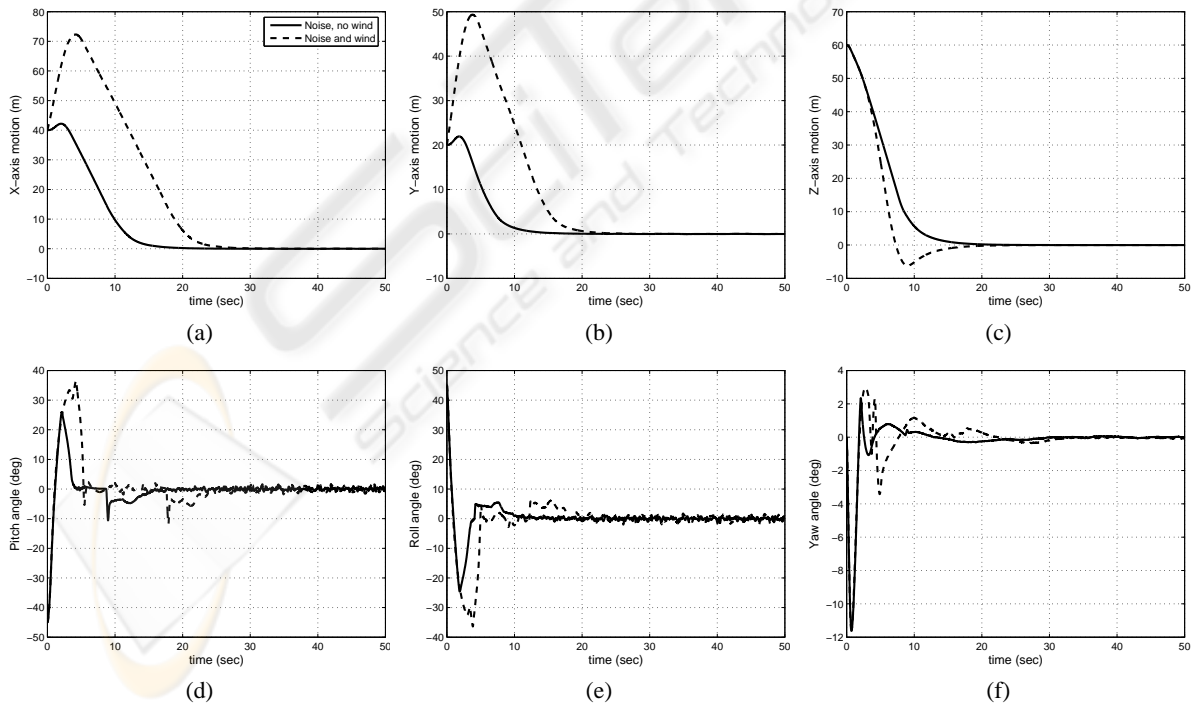

Figure 5: Experiment 2, Mamdani FLC's performance with a different initial condition. Quadrotor states: (a) x-axis; (b) y-axis; (c) z-axis (altitude); (d) pitch (θ); (e) roll (ϕ); and (f) yaw (ψ).
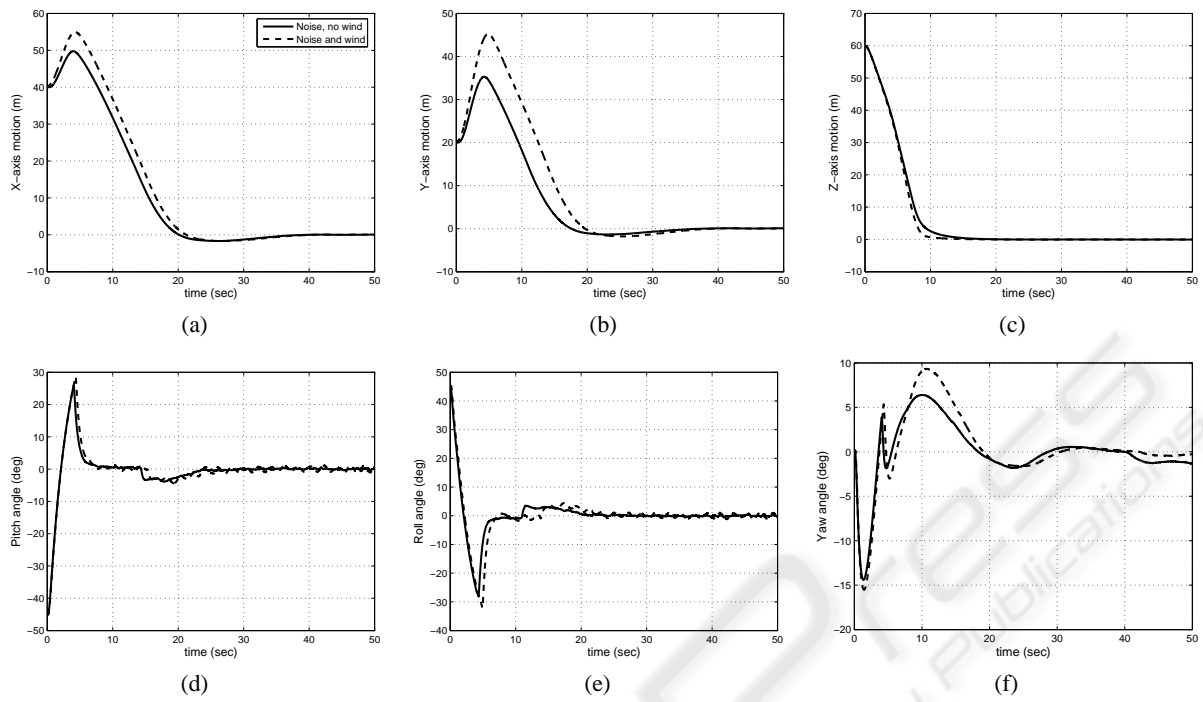
Figure 6: Experiment 2, Sugeno FLC's performance with a different initial condition. Quadrotor states: (a) x-axis; (b) y-axis;; (c) z-axis (altitude); (d) pitch (θ); (e) roll (φ); and (f) yaw (ψ).
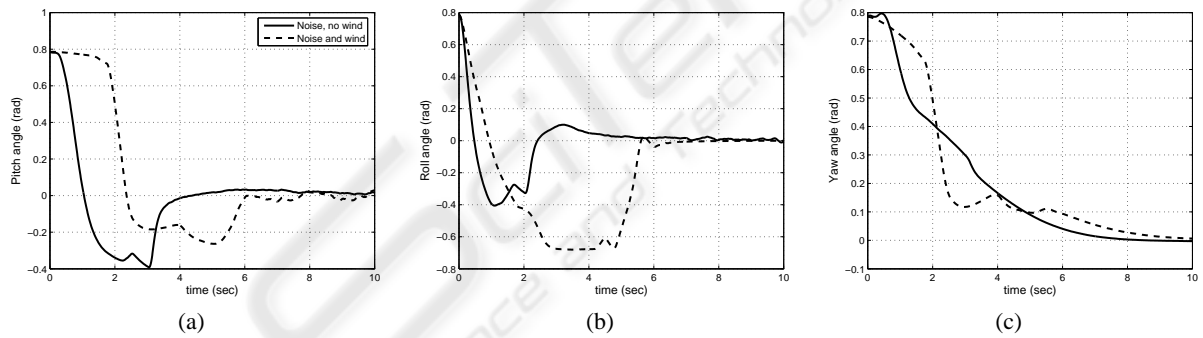

Figure 7: Experiment 3, Mamdani FLC's attitude stabilization. Quadrotor orientation: (a) pitch angle (θ); (b) roll angle (φ); and (c) yaw angle (ψ).
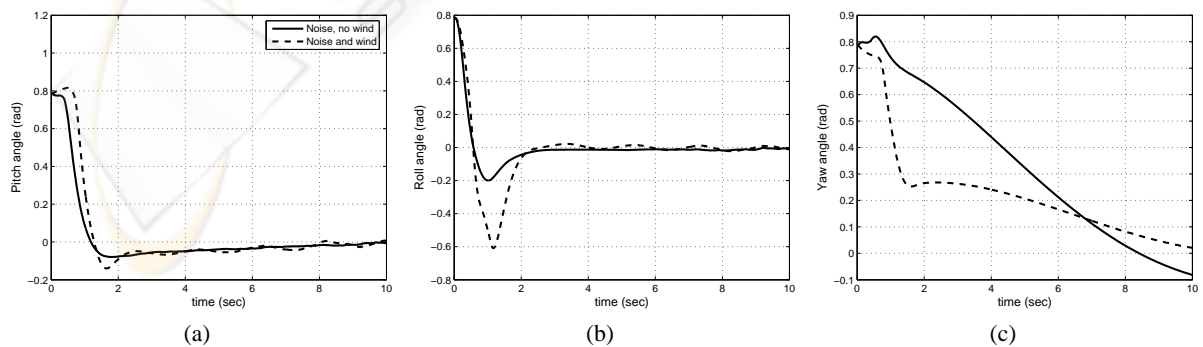

Figure 8: Experiment 3, Sugeno FLC's attitude stabilization. Quadrotor orientation: (a) pitch angle (θ); (b) roll angle (φ); and (c) yaw angle (ψ).

the performance of the fuzzy controllers as compared to a robust backstepping technique for nonlinear control in Figures 7, 8. Both Mamdani and Sugeno fuzzy controllers are able to stabilize the quadrotor from the critical initial conditions. The settling times are slightly longer than the backstepping controller, specially for the ψ angle which can be improved with further tuning of the FLC's membership functions. However, this is overlooked because the fuzzy controllers are stabilizing both position and attitude despite the presence of strong wind conditions as high as $30m/s$ and sensory noise of $-55dB$.

5 CONCLUSIONS

A fuzzy logic approach was proposed for the autonomous control of quadrotors without the need for a mathematical model of their complex and ill-defined dynamics. The fuzzy technique was implemented through Sugeno and Mamdani inference engines for comparison. The controller comprises of six individual fuzzy controllers designated for the control of the quadrotor's position and orientation. The investigation on the two types of control methodologies is conducted in a simulation environment, where disturbances such as wind conditions and sensor noise are incorporated for a more realistic simulation. The results demonstrated a successful control performance of the quadrotor with both Mamdani and Sugeno fuzzy controllers despite the disturbances. When compared with other control techniques presented in the literature for the same purpose, the proposed method showed a higher robustness and faster convergence, where satisfactory attitude stabilization is achieved despite stringent initial conditions and severe disturbances. The future work will be directed towards a real-world implementation of the proposed fuzzy controllers. Furthermore, the online adaptation of controllers will be investigated.

REFERENCES

Altug, E., Ostrowski, J., and Mahony, R. (2002). Control of a quadrotor helicopter using visual feedback. In *Proceedings of the 2002 IEEE International Conference on Robotics and Automation*, pages 72–77.

Bouabdallah, S., Murrieri, P., and Siegwart, R. (2004a). Design and control of an indoor micro quadrotor. In *Proceedings of the International Conference on Robotics and Automation*.

Bouabdallah, S., Noth, A., and Siegwart, R. (2004b). PID vs LQ control techniques applied to an indoor micro quadrotor. In *International Conference on Intelligent Robots and Systems*.

Coza, C. and Macnab, C. (2006). A new robust adaptive-fuzzy control method applied to quadrotor helicopter stabilization. In *Annual meeting of the North American Fuzzy Information Processing Society*, pages 454–458.

Dzul, A., Castillo, P., and Lozano, R. (2004). Real-time stabilization and tracking of a four-rotor mini rotor-craft. *IEEE Transaction on Control System Technology*, 12(4):510–516.

Fincannon, T., Barnes, L. E., Murphy, R. R., and Riddle, D. L. (2004). Evidence of the need for social intelligence in rescue robots. In *Proceedings of 2004 IEEE/RSJ International Conference on Intelligent Robots and Systems*, pages 1089–1095.

Guenard, N., Hamel, T., and Mahony, R. (2008). A practical visual servo control for an unmanned aerial vehicle. *IEEE Transactions on Robotics*, 24(2):331–340.

Guenard, N., Hamel, T., and Moreau, V. (2005). Dynamic modeling and intuitive control strategy for an X4-flyer. In *International Conference on Control and Automation*, pages 141–146.

Statistics, C. W. (2009). courtesy of environment canada. [Online] Available. http://www.weatherstats.ca/.

Tarbouchi, M., Dunfied, J., and Labonte, G. (2004). Neural network based control of a four rotor helicopter. In *International Conference on Industrial Technology*, pages 1543–1548.

Tayebi, A. and McGilvray, S. (2006). Attitude stabilization of a vtol quadrotor aircraft. *IEEE Transaction on Control System Technology*, 14(3):562–571.

Waslander, S. L., Hoffmann, G. M., Jang, J. S., and Tomlin, C. J. (2005). Multi-agent quadrotor testbed control design: integral sliding mode vs. reinforcement learning. In *International Conference on Intelligent Robots and Systems*, pages 468–473.